ECCOMAS Congress 2016
VII European Congress on Computational Methods in Applied Sciences and Engineering
M. Papadrakakis, V. Papadopoulos, G. Stefanou, V. Plevris (eds.)
Crete Island, Greece, 5–10 June 2016

IMPLEMENTATION OF PROGRESSIVE DAMAGE IN FINITE ELEMENT CODES FOR THE ASSESSMENT OF ROBUSTNESS

D. Asprone[1], **B. Chiaia**[2], **V. De Biagi**[2], **G. Manfredi**[1], **F. Parisi**[1]

[1]Università degli Studi "Federico II"
via Claudio 21, 80125 Napoli, Italy
e-mail: {d.asprone,g.manfredi,f.parisi}@unina.it

[2] Politecnico di Torino
C.so Duca degli Abruzzi 24, 10129, Torino, Italy
e-mail: {bernardino.chiaia,valerio.debiagi}@polito.it

Keywords: Robustness, Progressive Damage, Nonlinear FEM, Commercial software.

Abstract. *Different procedures for assessing the robustness of a reinforced concrete (RC) frame under progressive damage are proposed and compared. The removal of a column in a RC frame structure is modeled with a commercial nonlinear finite element software according to three alternative strategies: (i) reduction of mechanical properties of the damaged column, (ii) incremental loading of the structure after total removal of the damaged column, and (iii) incremental unloading of internal forces on the damaged column. Nonlinear analysis is performed under a prescribed load combination on three concrete frames designed with three Italian building codes in force in different periods. Despite the differences in the strategies for damage modeling, similarities between structural response predictions are highlighted. In addition, it is shown that seismic design provisions for RC building structures increase the ductility of the structure but do not guarantee the robustness against the removal of a column.*

1 INTRODUCTION

Structural engineers have been concerned with the resistance of building structures to disproportionate collapse since Ronan Point accident in 1968. In 2001, the catastrophic failures of WTC towers in New York showed the true effects of progressive collapse and raised the public interest on such topic. Specific guidelines have been developed and robustness requirements have been inserted in building codes and laws. Eurocode 0, which is the document at the base of the modern European national regulations on constructions, states that *a localised failure due to accidental actions may be acceptable, provided it will not endanger the stability of the whole structure, and that the overall load-bearing capacity of the structure is maintained and allows necessary emergency measures to be taken*.

In such framework, the researches conducted since the second half of the last century have focused the attention on sudden element removals [1, 2, 3]. Basically, such situations are induced by explosions and impact loads [4]. For ensuring structural robustness in constructions, the modern design philosophies switch from being reliability-based to accounting for consequences of local failure. In this sense, Gudmundsson and Izzuddin [5] argued that the scenario of sudden column loss is an effective and straightforward strategy for integrity assessment. Various design guidelines implement such approach through linear/nonlinear static or nonlinear dynamic analysis [6, 7]. On one side, static analysis with dynamic increase factor may lead to conservative rather than unsafe design depending on the structural behaviour and configuration [8]. On the other, a large computational effort is required for detailed nonlinear dynamic analyses [9].

Despite the previous scenario are the ones that have engendered and still cause many fatalities for building occupants, the attention has recently switched on other sources of degradation and damage [10, 11]. For example, Sun and others dealt with the progressive collapse of steel frames due to fire [12, 13] modifying a FEM code developed at the University of Sheffield. Others used commercial FEA software ABAQUS for investigating the behaviour of steel structures and connections subjected to fire loads, e.g., [14]. Fang and others [15] proposed a simplified energy-based robustness assessment approach in which the maximum temperature is unknown (i.e., this represents an event-independent local damage scenario); they assess the integrity of the steel structure subjected to fire through a multistage procedure implemented on ADAPTIC code.

The robustness of concrete buildings subjected to element removal has been usually assessed through numerical, experimental and analytical strategies (see, for example, [16, 17, 18]). In addition, theoretical [19, 20, 21, 22] and probabilistic approaches [23, 24, 25] as well as scenario analyses have been already formulated and proposed [26].

The aim of the research herein presented is to model in a simple and feasible way a progressive damage acting on concrete frame structure through a commercial software. This is fundamental for assessing the robustness of a construction in such unexpected scenarios [27].

2 METHODS

A progressive damage acting on a column of the first level of a reinforced concrete structure is simulated. The structure is subjected to the following load combination

$$1.50\,(DL + 0.25LL)\,, \tag{1}$$

where DL represents the dead load, i.e., the weight of the structural and nonstructural components; LL is the live load, i.e., the moving loads. This load combination is suggested in GSA

[28]; the term 1.50 is the dynamic amplification factor [29].

The test structure is represented by a 14×30 m reinforced concrete frame structure made of 140 beams and 160 columns distributed in five levels. The columns are disposed along the nodes of a grid, as depicted in the schematic of Figure 1(a). The plan position of each column is identified by means of a letter (from A to H) and a number (from 1 to 4) As can be observed in Figure 1(b), at each level, each node is connected with the neighboring ones through an orthogonal mesh of beams (28 beams per level). The levels are labelled by Roman numbers from I (ground level at +0.00 m) to VI (top level at +15.20 m). The interstorey height is 3.20 m for level II and 3.00 m for the remaining levels. The elevation of the levels is reported in Table 1. The bottom nodes, i.e., the foundation nodes, are rigidly constrained.

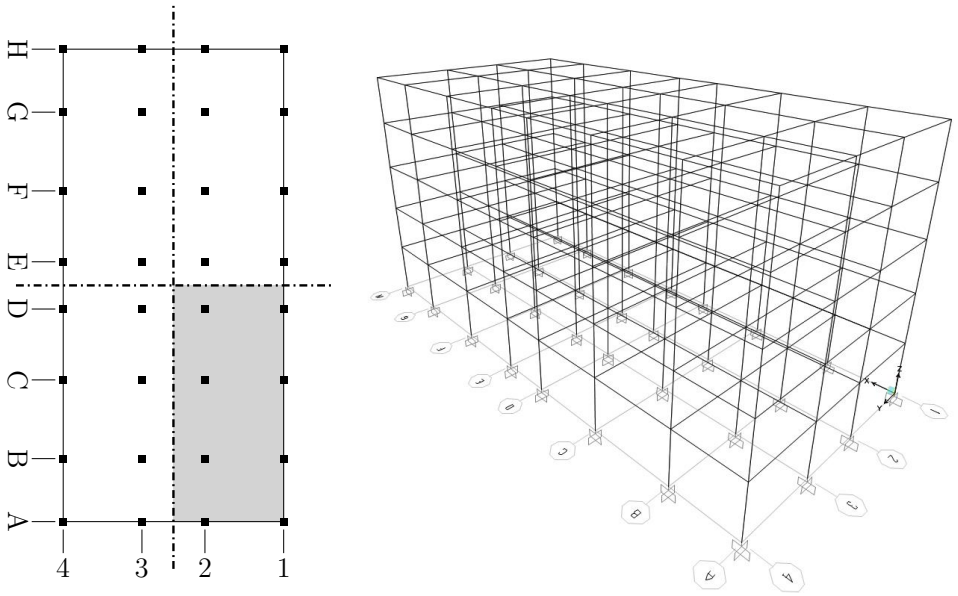

(a) (b)

Figure 1: (a) Plan view of the schematic of the reinforced concrete frame structure; (b) prospective of the frame structure.

Level	Elevation	Level	Elevation
I	0 m	IV	9.2 m
II	3.2 m	V	12.2 m
III	6.2 m	VI	15.2 m

Table 1: Elevations of the levels of the structure.

In the following, the nodes are identified by the sequence N:[plan position(level)]; for example, the node set at the fourth level at the position identified by letter E and number 3 is written as "N:E3(IV)". The beams are identified by the sequence B:[position of the initial node]:[position of the final node]; in this sense, for example, the beam of the third level (+9.20 m) connecting the nodes N:C2(III) and N:D2(III), is named as "B:C2(III):D2(III)". The columns are identified by the sequence C:[position of the bottom node]:[position of the top node]; for example, the column between the nodes N:F2(II) and N:F2(III) is denoted as "C:F2(II):F2(III)". The structure is doubly symmetrical in plan. Thus, the right-hand side lower quarter is considered in the present paper. The results are replicable to the other corresponding parts of the structure.

Referring to the amount of reinforcement within the elements, the structural safety (of the undamaged structure) has been guaranteed through three different design philosophies. In the first case (named "D+HoR" in the following), ultimate limit state semi-probabilistic approach accounting for ductility and hierarchy of resistances has been implemented; in the second case (named "D" in the following), only ductility requirements are satisfied; in the third case (named "S" in the following), only static design accounting for dead and live loads (with basic seismic design requirements) has been performed. The previous design philosophies correspond to present and early Italian building laws, i.e., [31], [32], [33], respectively. Following the well-known structural mechanics rules, the bending moment-curvature relationships for each of the three structural schemes previously illustrated has been computed and the nonlinear flexure relationships have been implemented in the corresponding Finite Element models.

The effects of progressive column removal have been analyzed through the implementation of three different numerical strategies, described in detail in the following subsections.

In all simulations, eight columns, corresponding to the bottom column of the studied quarter of the construction, are alternatively considered. The identification codes and sizes of the columns are reported in Table 2. The behavior of the structure to the progressive damage is evaluated through the maximum vertical drift of all the beams converging in the top node of the damaged element. In reference to Figure 2 in which two horizontal beams converge in node N, the vertical drift, v_{N}, is

$$v_{\mathrm{N}} = \max\left\{\frac{\Delta_1}{\ell_1}; \frac{\Delta_2}{\ell_2}\right\}. \tag{2}$$

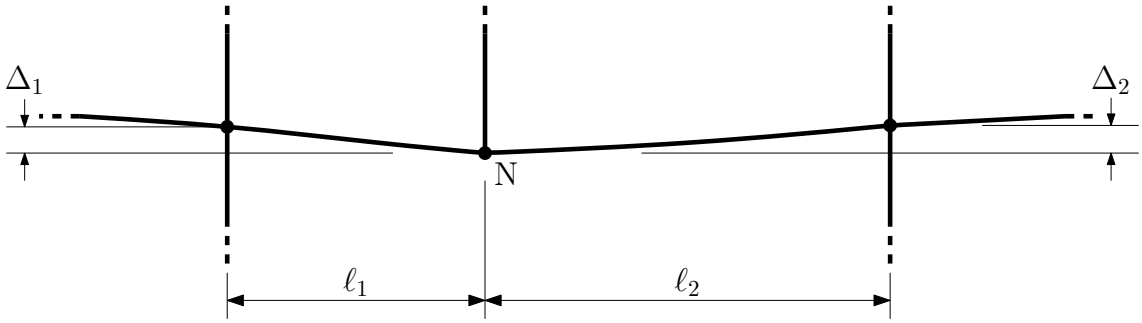

Figure 2: Scheme for the evaluation of vertical drift.

Progressive number	Identification code	Size (cm^2)	Progressive number	Identification code	Size (cm^2)
#1	C:A1(I):A1(II)	30x50	#5	C:A2(I):A2(II)	30x65
#2	C:B1(I):B1(II)	60x30	#6	C:B2(I):B2(II)	65x40
#3	C:C1(I):C1(II)	60x30	#7	C:C2(I):C2(II)	65x40
#4	C:D1(I):D1(II)	50x30	#8	C:D2(I):D2(II)	30x60

Table 2: Damaged elements.

The simulations were performed on an Intel i7, 3.60 GHz, 64-bit computer with 16 GB RAM. A specific MATLAB script controlled a SAP2000 solver and stored the displacement of the monitored nodes on a database file. The computation times related to each simulation are evaluated through MATLAB software.

2.1 Damage model A

The damage model A implemented a progressive reduction of the cross-section area and inertia. As implemented by Lematre and Chaboche [30], the degradation of the structural element was controlled by a damage parameter d varying from 0, in case of no damage, to 1, in case of total damage. If $d = 1$ the element is totally removed. The geometrical properties of the i-th element, i.e., the damaged element, of the RC frame were

$$\begin{aligned} A_{id} &= A_{i0}\,(1-d) \\ J_{id} &= J_{i0}\,(1-d)^2\,, \end{aligned} \tag{3}$$

where A_{i0} and J_{i0} are the cross-section area and inertia. The damage model acted on the size of the concrete cross section, not on the area of the rebar.

The eight columns previously identified were alternatively subjected to the damage, and the overall response of the frame structure was monitored. The simulations (21 in total) were performed at the following values of the damage parameter d:

- from d = 0.000 to d = 0.700, with step of 0.100;
- from d = 0.700 to d = 0.850, with step of 0.050;
- from d = 0.850 to d = 0.950, with step of 0.025;
- from d = 0.950 to d = 0.990, with step of 0.010;
- at d = 0.995 and d = 1.000.

For each value of the damage parameter, the reduced geometrical properties, i.e., the ones derived from Eqn. (3), are automatically assigned to the damaged element. For sake of simplicity, a unique undamaged scheme was considered as a basis for all the simulations. The external load was applied to the damaged structure with its nominal value, see load combination detailed in Eqn. (1). SAP2000 solver was set as static nonlinear. Meanwhile, the vertical displacements of the top node of the damaged column (i.e., the node set at level II, i.e., at +3.20 m), as well as the boundary nodes at the same level, were monitored. In addition, the axial force in the damaged element was recorded. This allowed to rapidly estimate the vertical drift of the beams at +3.20 m, assessing the amount of damage on the floor. The results associated with each value of damage parameter were independent one from each other. No previous damage history is considered was each simulation.

2.2 Damage model B

The damage model B considered the total removal of the damaged element and the progressive loading of the structure. Before the incremental loading of the structure, no additional loads were acting on the scheme. The loading process was controlled by the vertical displacement of the top node of the damaged element (i.e., the node set at +3.20 m). Because of that, the loading process might be related to an incremental "pushdown" analysis. In order to monitor the effective load on the structure at each loading step, the total base vertical reaction was considered. The reference base reaction value in the undamaged scheme was determined before the removal of the element and, then, the corresponding values at each loading step were recorded.

2.3 Damage model C

The damage model C considered the substitution of the damaged element with a set of forces that simulate its presence. The forces are then progressively reduced to zero. The simulations accounting for this damage model were implemented as follows, see Figure 3 for visual details. First, (i) the undamaged structure was loaded with the external loads with the load combination into Eqn. (1). A nonlinear solver was considered and the displacements and the forces in the elements were evaluated. In particular, the forces acting in the potentially damaged element were recorded, i.e., the red forces in Figure 3(a). In the present paper, only the forces acting at the top end of the element were considered; the bottom end of the element, being a base column, was restraint. Then, (ii) the damaged element was removed and a set of external forces, F^*, were added to the scheme, black forces in Figure 3(b). Such forces are opposite to the ones of the previous step, i.e., $F^* = -F$. A nonlinear run was made and the nodal displacements were read and it resulted that were approximatively equal to the ones computed at step (i). In the following (iii), a system of forces f opposite to the ones derived in the previous step (ii) was added on the node, as sketched in blue in Figure 3(c). The purpose of the model was to progressively reduce the effects of forces F^*, which means damaging the i-th element. Thus, forces f were progressively increased from zero to F following a displacement controlled incremental scheme (see Damage model B for details on the control node). Therefore, it results

$$\begin{aligned} f &: 0 \to F \\ F^* + f &: F^* \to 0. \end{aligned} \tag{4}$$

It might happen that it was not possible to increment the forces f to their nominal value F because a failure occurs in the loading process. In this case, the ultimate value of f was considered in the analysis.

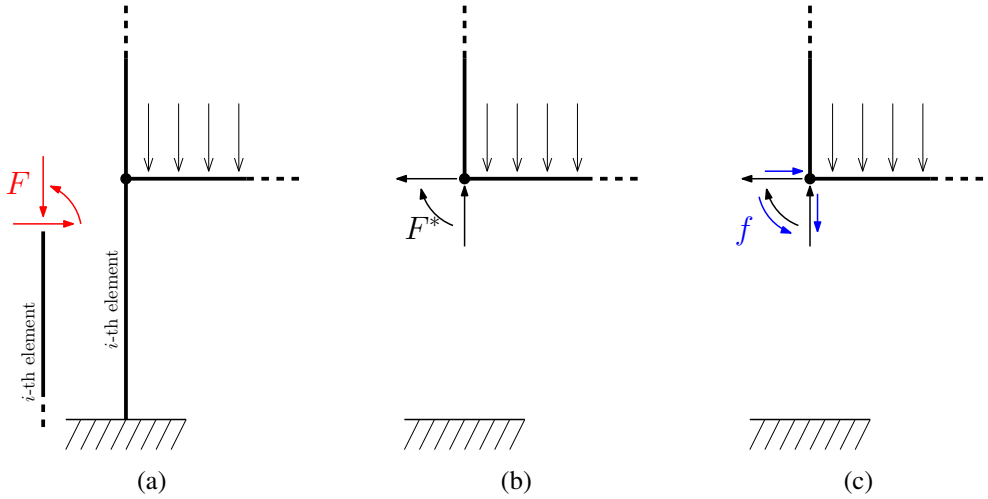

Figure 3: Damage model C. The details are reported in section 2.3.

3 RESULTS

The observed behavior modes of the three structures subjected to the three damage models are presented in the following. Figure 4 displays the values of vertical drift as much as the

damage parameter d increases. If figure panels are observed, it emerges that the trends obtained for the three structures designed with different standards ("S", "D" or "D+HoR") are similar. The increment of the vertical drift is relatively small for low values of damage parameter, while it sharply increases as much as d tends to unity. The behaviors of the three different structures to damage are compared observing the ranges of the damage parameter at equal vertical drift. For the structure able to support static loads only, see Figure 4(a), a vertical drift of 10^{-3} is given for values of d ranging between 0.65 and 0.85 (depending from the damaged element). A narrow range of values of the damage parameter are found for the same vertical drift in the other two structures: 0.84 – 0.91 in ductile only schemes ("D") and 0.86 – 0.92 in "D+HoR" structures.

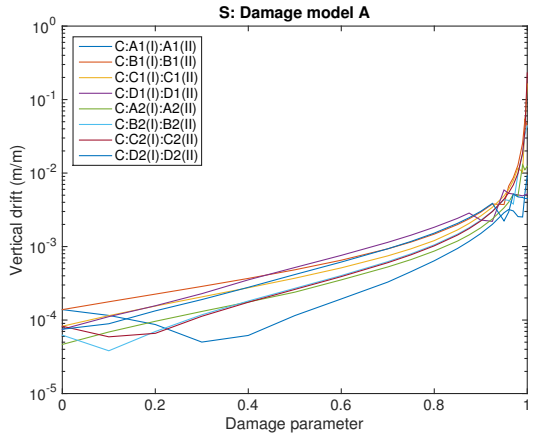

(a) "S": static design

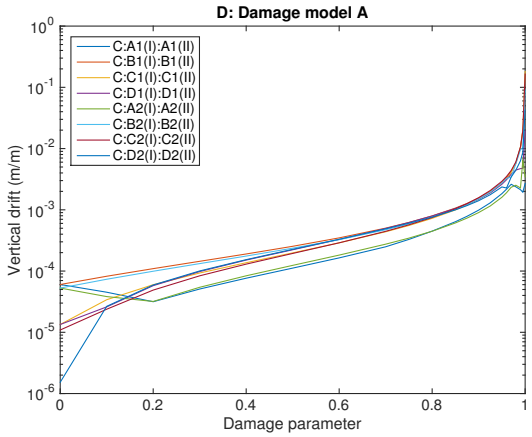

(b) "D": ductility design

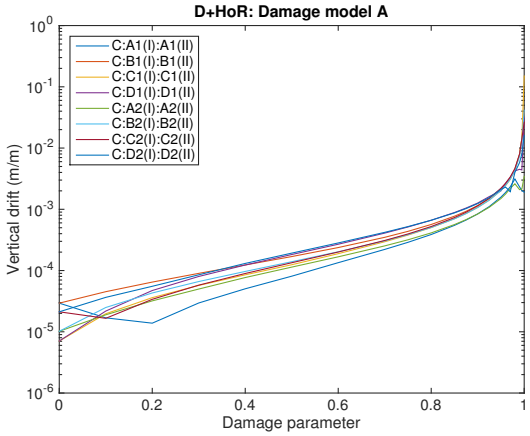

(c) "D+HoR": ductility + hierarchy of resistances design

Figure 4: Vertical drifts as functions of the damage parameter d for the Damage model A.

Figure 5 gives the outputs of pushdown analysis illustrated in the framework of Damage model B. The loading percentage is plotted with reference to the vertical drift. It is observed that the overall response varies depending on the structural design and on the damaged element. In none of the considered cases, the values attain 100%, i.e., it is not possible to apply on the structure the loading combination reported in Eqn. (1). The inspection of Figure 5(a) indicates that the response of the structure "S" is variable: the maximum loading allowed on the damaged scheme is about 50% in case of the removal of column C:A2(I):A2(II). Lower values, i.e.,

between 25% and 30% of the nominal loading expressed by Eqn. (1), are found in case of damage of the remaining elements. Different trends are observed for the structures designed with ductility. The behaviors of "D" and "D+HoR" schemes under damage are essentially the same. The maximum loading related to the tests performed on columns C:D1(I):D1(II) and C:D2(I):D2(II), i.e., the violet and blue curves in Figures 5(b) and 5(c), is larger than 80% of the nominal value. In the tests performed on the other columns, the maximum load ranges between 40% and 60%. The plateau in some curves on "D" and "D+HoR" structures confirm that, before failure, plastic hinges form and the structure dissipate energy in order to support larger loads.

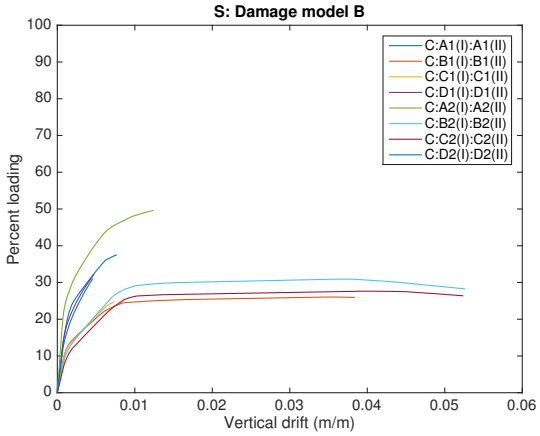

(a) "S": static design

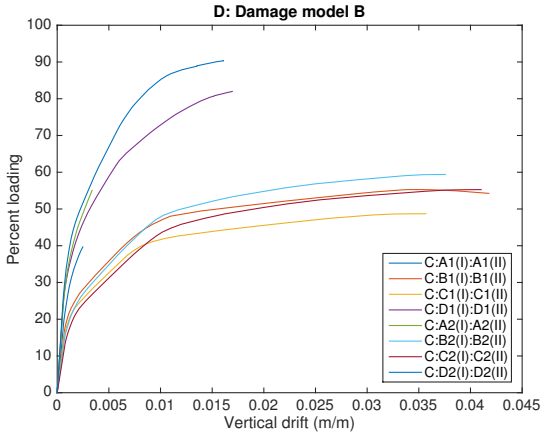

(b) "D": ductility design

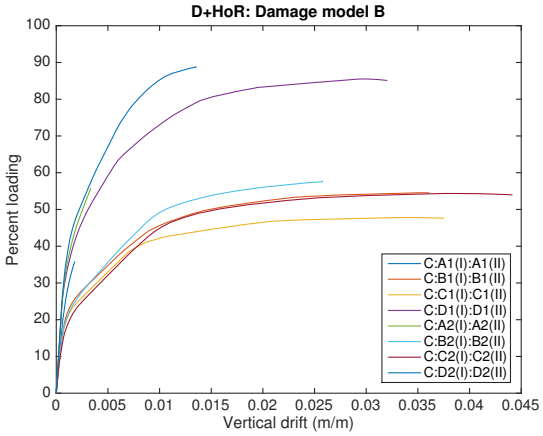

(c) "D+HoR": ductility + hierarchy of resistances design

Figure 5: Vertical drifts and percentage of unloading for Damage model B.

Consistent results are found if Damage model C (Figure 6) is considered. Despite the loading on the structure is different from the previous damage model, the results are quite similar. The tests conducted on the structure designed to support static loads show that the unloading ranges between 20% and 50%, as displayed in Figure 6(a). Meanwhile, the remaining schemes confirm that it is not possible to add the nominal value of f in order to set to cancel the force F^*. Ranges between 40% and 90% are observed in Figures 6(b) and 6(c).

Both Damage model B and C identify the behavior of the damaged structure through values of vertical drift and loading/unloading percentages. Therefore, a relationship between the two

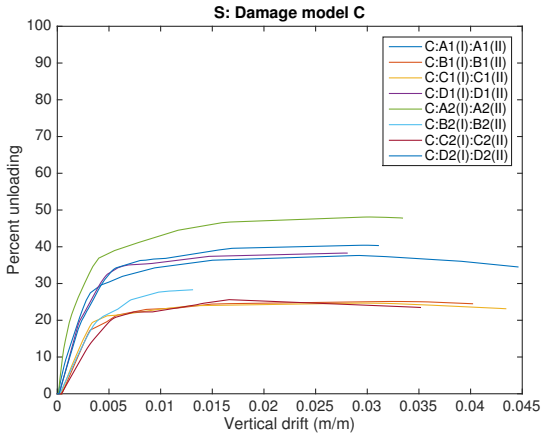

(a) "S": static design

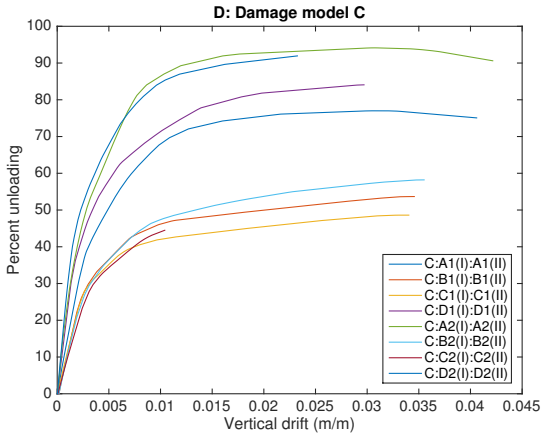

(b) "D": ductility design

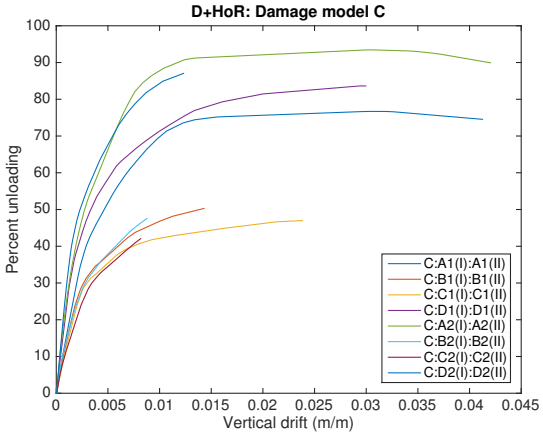

(c) "D+HoR": ductility + hierarchy of resistances design

Figure 6: Vertical drifts and percentage of loading for Damage model C.

different approaches is investigated. The coupling between the results of the two damage models is made through the value of the vertical drift. The loading percentages of Damage model B are interpolated at the values of the drifts corresponding to the computed unloading percentages of Damage model C. In Figure 7 the correlation points are plot. It results that at 0% in Damage model B, positive percentages are evaluated in Damage model C. This is due to the fact that at the beginning of the simulation in Damage model B the structure is unloaded, i.e., no vertical drift is recorded, while it is loaded (and, thus, deformed) at the initial step of the simulations with Damage model C.

Fair correlation is seen in any of the considered structures for loading/unloading percentages smaller than roughly 35%. In the schemes designed with ductility requirements (i.e., both "D" and "D+HoR") better results are observed in some tests for percentages larger than 50%.

In order to assess the computational effort for performing the simulations, the computation times needed for getting the results herein presented have been recorded. As emerges in Table 3, the time needed for the calculations related to Damage model A is one order of magnitude larger than the one necessary to perform the robustness analysis on Damage models B and C.

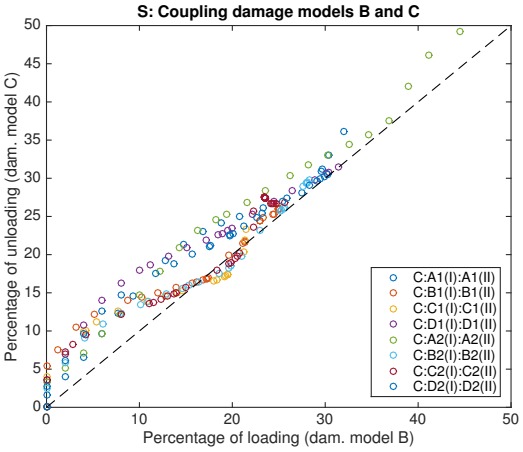

(a) "S": static design

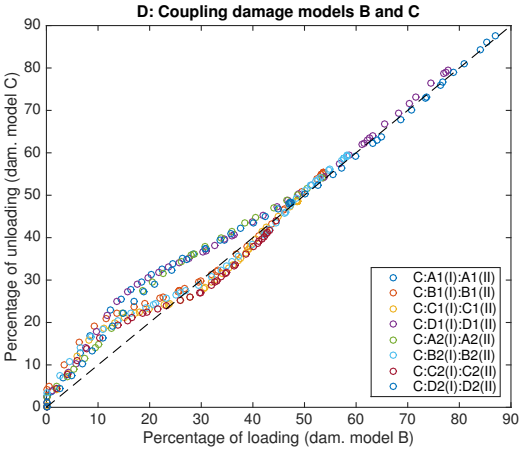

(b) "D": ductility design

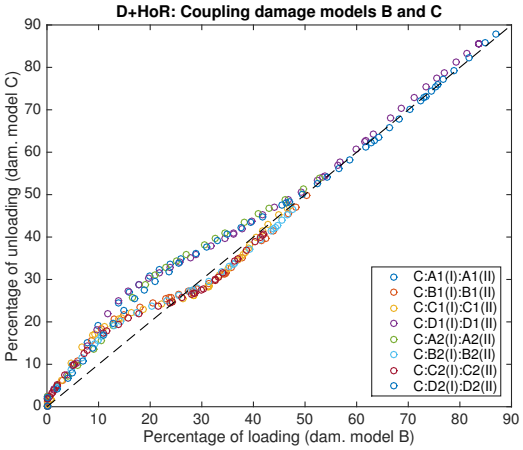

(c) "D+HoR": ductility + hierarchy of resistances design

Figure 7: Coupling between Damage model B and Damage model C. The dashed line is the bisector of the quarter, identifying the perfect correlation between the two damage models.

4 DISCUSSION AND CONCLUSIONS

A literature overview has highlighted that no detailed researches were conducted on the ways to implement a damage condition in a commercial FEM software in order to assess the structural robustness of a construction. The present approach deals with three different strategies that do not expressly consider the damage from a local (microscopic effects on the damaged element) to a global (the whole construction) scale. The first damage model evaluates the response of the structure for various levels of cross-section reduction in selected damaged elements. The second damage model presupposes that selected elements are removed and the structure is incrementally loaded. In the last damage model, the damaged element is replaced by an additional system of forces equivalent to the ones that it experiences in the undamaged structure; then, forces are progressively reduced. In real situations, the external loads (gravity + dead load) are always present throughout all the duration of the damage process. Because of that, we think that Damage model C can provide a good representation of what might happen on a real damaged structure. Meanwhile, we observe that a damage on a column is monitored through geometrical and mechanical data (carbonation depth, spalling, aging): in this case, there are no clear connec-

Scheme	Dam. model A	Dam. model B	Dam. model C
S	6h 12m	0h 24m	0h 31m
D	5h 52m	0h 38m	0h 37m
D+HoR	3h 40m	0h 27m	0h 17m

Table 3: Computation times.

tions between the percentage of unloading and the amount of damage on the element. Although Damage model A tries to overcome this problem through the damage parameter, its inadequacy is highlighted by the fact that at the beginning of each simulation the structure is unloaded. Damage model B does not consider neither the presence of the element during the damage process nor the loads acting on the structure. However, it is the simplest to be implemented in the analysis since no iterative calculations or advanced modeling are required.

We believe that the Damage model C can be the most accurate among the three proposed strategies for assessing the structural robustness of a structure. However, at present, its implementation in a commercial code is not simple because programming abilities are required. Usually, softwares does not allow to control single loadcases, except those related to seismic horizontal force in push-over analyses. The implementation of Damage model C in the commercial softwares would require a specific plug-in able to perform such kind of analyses.

Anyway, the results of Damage models B and C are comparable, as found in Figure 7. That is why we believe that Damage model B, which is the simplest and the quickest to be implemented among the three proposed strategies, can give insights on the structural robustness of a scheme. This choice is supported by the fact that there are no substantial differences in the computational effort in choosing Damage model B or C for assessing the robustness of the structure.

In general, we found that none of the three structures designed with different standard requirements are safe in case of the removal of a column at the bottom level. This confirms that seismic design guidelines and principles do not necessarily ensure the structural robustness of a building.

Future developments of the research would deal with the correlation between the physical damage and the parameters to be used in the numerical simulation. This would permit to assess the reliability of a structure onto which a progressive damage is acting.

ACKNOWLEDGEMENTS

The present work was done under in framework of ReLUIS project 2014/2016 “Supporto alle attività di gestione tecnica dell’emergenza e connesse ai programmi di prevenzione sismica, per lo sviluppo della conoscenza e l’assistenza alla redazione di norme tecniche, per la collaborazione alle attività di formazione, comunicazione e divulgazione – ReLUIS. Linea di ricerca Cemento Armato”.

REFERENCES

[1] J. Kim, T. Kim. Assessment of progressive collapse-resisting capacity of steel moment frames. *Journal of Constructional Steel Research*, **65**,169–179, 2009.

[2] B.A. Izzuddin, A.G. Vlassis, A.Y. Elghazouli, D.A. Nethercot. Progressive collapse of multi-storey buildings due to sudden column loss? Part I: simplified assessment framework. *Engineering Structures*, **30**, 1308–1318, 2008.

[3] A.G. Vlassis, B.A. Izzuddin, A.Y. Elghazouli, D.A. Nethercot. Progressive collapse of multi-storey buildings due to sudden column loss? Part II: application. *Engineering Structures*, **30**, 1424–1438, 2008.

[4] F. Parisi, C. Balestrieri, D. Asprone. Blast resistance of tuff stone masonry walls. *Engineering Structures*, **113**, 233–244, 2016.

[5] G.V. Gudmundsson, B.A. Izzuddin. The 'sudden column loss idealisation' for disproportionate collapse assessment. *The Structural Engineer*, **88**, 22–26, 2010.

[6] British Standards Institution. *BS 5950: Structural use of steelwork in buildings, Part 1: code of practice for design ? rolled and welded sections*. London, 2001.

[7] Unified Facilities Criteria. *Design of buildings to resist progressive collapse*. Department of Defense, Virginia, USA, 2009.

[8] H. Zolghadr Jahromi, A.G. Vlassis, B.A. Izzuddin. Modelling approaches for robustness assessment of multi-storey steel-composite buildings. *Engineering Structures*, **51**, 287–294, 2013.

[9] L. Kwasniewski. Nonlinear dynamic simulations of progressive collapse for a multistory building. *Engineering Structures*, **32**, 1223–35, 2010.

[10] D. Asprone, F. Jalayer, A. Prota, G. Manfredi. Proposal of a probabilistic model for multi-hazard risk assessment of structures in seismic zones subjected to blast for the limit state of collapse. *Structural Safety*, **32**, 25–34, 2010.

[11] E. Nigro, A. Bilotta, D. Asprone, F. Jalayer, A. Prota, G. Manfredi. Probabilistic approach for failure assessment of steel structures in fire by means of plastic limit analysis. *Fire Safety Journal*, **68**, 16–29, 2014.

[12] R.R. Sun, Z.H. Huang, I.W. Burgess. Progressive collapse analysis of steel structures under fire conditions. *Engineering Structures*, **34**. 400–413, 2012.

[13] R.R. Sun, Z.H. Huang, I.W. Burgess. The collapse behaviour of braced steel frames exposed to fire. *Journal of Constructional Steel Research*, **72**, 130–142, 2012.

[14] K.T. Ng, L. Gardner. Buckling of stainless steel columns and beams in fire. *Engineering Structures*, **29**, 711–30, 2007.

[15] C. Fang, B.A. Izzuddin, A.Y. Elghazouli, D.A. Nethercot. Simplified energy-based robustness assessment for steel-composite car parks under vehicle fire. *Engineering Structures*, **49**, 719–732, 2013.

[16] J.L. Le, B. Xue. Probabilistic analysis of reinforced concrete frame structures against progressive collapse. *Engineering Structures*, **76**, 313–323, 2014.

[17] S. Sagiroglu, M. Sasani. Progressive collapse-resisting mechanisms of reinforced concrete structures and effects of initial damage locations. *Journal of Structural Engineering*, **140**, 04013073-1–12, 2014.

[18] A. Fascetti, K.S. Kunnath, N. Nisticò. Robustness evaluation of RC frame buildings to progressive collapse. *Engineering Structures*, **86**, 242–249, 2015.

[19] V. De Biagi, B. Chiaia. Complexity and robustness of frame structures. *International Journal of Solids and Structures*, **50**, 3723–3741, 2013.

[20] C. Cennamo, B. Chiaia, V. De Biagi, L. Placidi. Monitoring and compartmentalized structures. *Zeitschrift für Angewandte Mathematik und Mechanik*, **95**, 638–648, 2015.

[21] V. De Biagi. Structural behavior of a metallic truss under progressive damage. *International Journal of Solids and Structures*, **82**, 56–64, 2016.

[22] V. De Biagi, B. Chiaia. Damage tolerance in parallel systems. *International Journal of Damage Mechanics*, 1–20, 2016. (DOI: 10.1177/1056789516630777)

[23] P. Russo, F. Parisi. Risk-targeted safety distance of reinforced concrete buildings from natural-gas transmission pipelines. *Reliability Engineering and System Safety*, **148**, 57–66, 2016.

[24] E. Brunesi, R. Nascimbene, F. Parisi, N. Augenti. Progressive collapse fragility of reinforced concrete framed structures through incremental dynamic analysis. *Engineering Structures*, **104**, 65–79, 2015.

[25] F. Parisi F. Blast fragility and performance-based pressure?impulse diagrams of European reinforced concrete columns. *Engineering Structures*, **103**, 285–297, 2015.

[26] F. Parisi, N. Augenti. Influence of seismic design criteria on blast resistance of RC framed buildings: a case study. *Engineering Structures*, **44**, 78–93, 2012.

[27] V. De Biagi, B. Chiaia, B. Frigo. Impact of snow avalanche on buildings: Forces estimation from structural back-analyses. *Engineering Structures*, **92**, 15–28, 2015.

[28] General Services Administration, *Alternate Path Analysis & Design Guidelines For Progressive Collapse Resistance*. Washington, DC, 2013.

[29] P. Ruth, K.A. Marchand, E.B. Williamson. Static equivalency in progressive collapse alternate path analysis: reducing conservatism while retaining structural integrity. *Journal of Performance of Constructed Facilities*, **20**, 349–364, 2006.

[30] J. Lemaître, J.-L. Chaboche, *Mechanics of Solid Materials*. Cambridge University Press, 1994.

[31] Repubblica Italiana, Decreto Ministeriale 14/01/2008 – Norme tecniche per le costruzioni. *Gazzetta Ufficiale della Repubblica Italiana*, **29**, S.O. 30, 2008

[32] Repubblica Italiana, Decreto Ministeriale 16/01/1996 – Norme tecniche relative ai criteri generali di verifica di sicurezza delle costruzioni e dei carichi e sovraccarichi. *Gazzetta Ufficiale della Repubblica Italiana*, **29**, S.O. 19, 1996.

[33] Regno d'Italia, Regio decreto-legge 3/04/1930 – Nuove norme tecniche ed igieniche di edilizia per le localit sismiche. *Gazzetta Ufficiale del Regno di Italia*, **133**, 2236–2258, 1930.